Macromolecules

pubs.acs.org/Macromolecules
Article

Spin Relaxation and Dynamics of Ring Poly(ethylene oxide) in Melts

Kevin Lindt, Nail Fatkullin, Carlos Mattea, Jürgen Allgaier, Siegfried Stapf,* and Margarita Kruteva*

Cite This: Macromolecules 2024, 57, 3765−3775

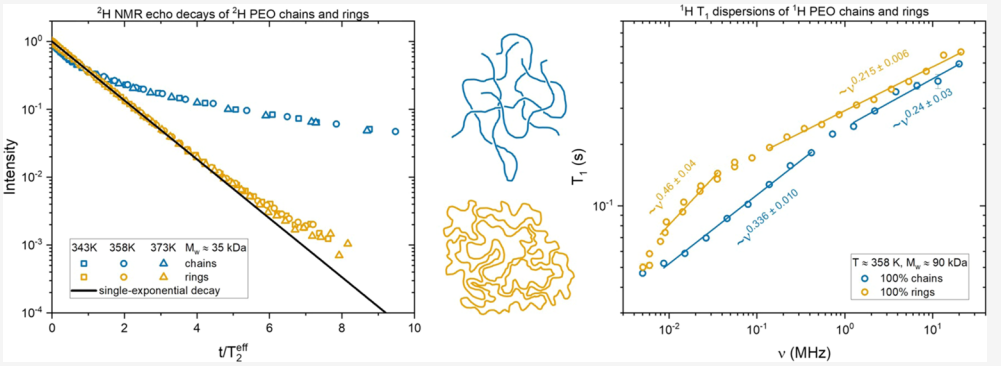

ABSTRACT: The spin relaxation of protons and deuterons was investigated in melts of ring poly(ethylene oxide) (PEO) macromolecules with a molecular mass varying from 5280 to 96,000 Da. Comparison of the frequency dispersion of NMR spin−lattice relaxation rates with corresponding rates in the melts of linear PEO of similar molecular masses shows that there is a significant mutual interpenetration of neighboring ring macromolecules, although less pronounced than in their linear counterparts. The mean-squared displacement of ring segments in the investigated frequency interval corresponding to the time interval 8×10^{-9} to 2×10^{-5} s depends on time as $\langle r_n^2(t)\rangle \propto t^{0.39}$, in agreement with neutron spin echo (NSE) results. Decays of the normalized Hahn echo signal in ring macromolecules are exponential within experimental errors, unlike for their linear counterparts where strongly nonexponential behavior is found. This indicates the absence of dynamic heterogeneity of ring segments seen by NMR and associated with the presence of end segments in their linear analogues.

INTRODUCTION

Although various properties of ring macromolecules started to be discussed several decades ago (see refs 1,2 and the literature cited therein), their systematic, experimental studies have begun relatively recently, and an understanding of their structural and dynamic properties still seems to be far from complete.[3−15] A fundamental and quantifiable property of ring macromolecules is the difference in their conformation in comparison to their linear analogues: The statistical distribution of conformations of linear macromolecules consisting of N Kuhn segments for sufficiently large N can be approximated with good accuracy as the distribution of a freely jointed ideal chain, and its gyration radius is equal to $R_g^{lin} = \sqrt{\left(\frac{N}{6}\right)}\, b$, where b is the length of a Kuhn segment.[16−20] Ring macromolecules in a melt have a significantly more compact globular structure with a radius of gyration that, for large N, depends on N as $R_g \propto bN^{1/3}$. This asymptotic behavior was found by numerical simulations,[7,13,21] but has never been verified experimentally.[3,10] The interaction between the intramolecular segments of macromolecules is equivalent to the interaction with segments of neighboring macromolecules. Therefore, the surface tension of globules formed by ring macromolecules is zero, and the globules do not have a distinct spatial shape. There is a broad, though on average spherically symmetric, distribution of possible spatial compact globular shapes, which possess strongly fluctuating compact porous structures as noted in ref 15.

The compact globular structure of the rings, *i.e.*, the linear size being smaller than the comparable freely joined analogue, seriously complicates the possibility of an analytical description of their dynamics. Indeed, in contrast to linear chains where a Gaussian distribution can be assumed, the distribution of ring conformations deviates from the Gaussian distribution on the length scale of an order of R_g.[10]

Therefore, the possible equations of motion of ring macromolecules become nonlinear, even at the level of intramolecular interactions. In addition, all of the difficulties associated with the effects of intermolecular entanglements

Received: November 17, 2023
Revised: February 18, 2024
Accepted: March 25, 2024
Published: April 9, 2024

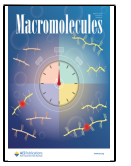

https://doi.org/10.1021/acs.macromol.3c02360
Macromolecules 2024, 57, 3765−3775

remain, which makes a complete analytical description of even the dynamics of melts of linear macromolecules, in our opinion, very far from being completed on all spatial and temporal scales. In this regard, theoretical results related to the dynamics of ring macromolecules are mainly (with the exception of refs 5,6) based on scaling arguments or on computer simulation data.

Experimental studies of the dynamics of ring macromolecules in melts were performed by neutron scattering,[10−12,22,23] rheology,[24,25] and pulsed field gradient NMR.[12,22] Microscopic dynamics of polymers is accessible by neutron scattering, in particular by the neutron spin echo (NSE) spectroscopy,[26] on a time scale up to 10^{-6} s allowing, due to the measurements in the Q-space, to resolve the displacements on a nanometer length scale. Pulsed field gradient (PFG) NMR operates in the time window between 10^{-3} and 1 s, covering length scales essentially larger than the ring size.

Combining NSE with (PFG) NMR, the topology driven self-similar internal ring dynamics predicted by the Fractal Loopy Globule (FLG) model[4] could be verified experimentally.[10−12] We find the center of mass diffusion $\langle r^2_{com}(t)\rangle$ taking place in three dynamic regimes from short to long times: (i) a strongly subdiffusive regime, *i.e.*, with time exponent $\alpha < 1$, $\langle r^2_{com}(t)\rangle \sim t^{\alpha}(0.4 \le \alpha \le 0.6)$, limited by $\langle r^2_{cross,1}\rangle \approx R^2_g$, (ii) a second regime $\langle r^2_{com}(t)\rangle \sim t^{0.75}$ that (iii) at $\langle r^2_{cross,2}\rangle \approx 2.5R^2_g$ crosses over to Fickian diffusion. While the second anomalous diffusion regime has been found in simulations and was predicted by theory, we attribute the first one to the effect of cooperative dynamics resulting from the correlation hole potential,[27] *i.e.*, the effective potential of interaction of two macromolecules with fixed positions of their center of mass. The internal dynamics at scales below the elementary loop size are well-described by Rouse motion. At larger scales, the dynamics is self-similar and follows very well the predictions of the scaling models with preference for the FLG model.

However, to date, to the best of our knowledge, there are no works in which the dynamics of ring macromolecules in melts have been studied employing spin−lattice and spin−spin relaxation NMR methods. Meanwhile, the spin-relaxation NMR methods are widely used to study the dynamics of melts of linear macromolecules and allow obtaining unique information inaccessible to other expert methods (see, for example, refs 28−30 and the literature cited therein).

In most general terms, spin−lattice, or longitudinal, T_1 relaxation is the establishment of thermodynamic equilibrium in the spin system of a sample along the orientation of the external magnetic field B_0. The characteristic time T_1 of this process depends on the resonance frequency associated with a constant external magnetic field by the ratio $\omega_0 = \gamma B_0$, where γ is the gyromagnetic ratio of the investigated nuclei. The relaxation processes are induced by thermal spatial displacements of the atoms surrounding the studied spin. These displacements cause a modulation of the local electromagnetic field, ultimately leading to spin relaxation. The abovementioned frequency dependence therefore carries information about dynamic processes at times of order ω_0^{-1}. Modern NMR spin−lattice relaxometry techniques allow the resonance frequency to be varied within 10^4−10^9 s^{-1}, *i.e.*, in corresponding time domain 10^{-9} to 10^{-4} s. Spin−spin or transverse T_2 relaxation represents the establishment of thermodynamic equilibrium in a plane perpendicular to the external permanent magnetic field. In melts of high molecular weight polymers, the characteristic spin−spin relaxation time T_2 is usually on the order of 10^{-3} s.

The main goal of this work is to investigate the dynamics of accessible melts of ring macromolecules by spin-relaxation NMR methods and to fill the abovementioned gap in the experimental data. Poly(ethylene oxide) (PEO) rings with molecular weight in the range from 5280 to 96,000 Da were used, and the frequency dependence of the relaxation times T_1 and T_2 was measured. Intramolecular contributions to the proton spin−lattice relaxation rate are independent of the proton concentration, while the intermolecular contributions are proportional to this concentration. This fact makes it possible to experimentally separate the discussed contributions by diluting protonated macromolecules in deuterated macromolecules having the same degree of polymerization. In order to separate intramolecular and intermolecular contributions to relaxation, deuterated PEO rings were explored.

THEORETICAL CONSIDERATION

The origin of NMR spin relaxation is the internal electromagnetic field generated by molecules as a whole and their fragments in the substance under study. Due to thermal molecular motions, these fields appear time-dependent, which induces quantum-mechanical transitions between different spin states in the external magnetic field and eventually leads the spin system to a state of thermal equilibrium (see more detailed discussions in refs 28−30 and numerous literature studies cited therein). At the initial stage of experiments, the spin system is in a state of thermodynamic equilibrium with the other degrees of freedom of the system under study, called in the magnetic resonance community the general term "lattice". Then, by means of special radiofrequency pulses, the spin system is perturbed from its initial thermodynamic equilibrium state. The rate at which the thermodynamic equilibrium is restored in the studied spin system due to the abovementioned processes turns out to depend on the relative spatial displacements of spin-carrying atomic nuclei.

Proton nuclei possess spin $I = 1/2$ and therefore have zero quadrupole moment. The dominant interactions determining the spin relaxation of protons in the absence of additional electron paramagnetic impurities are, as a rule, magnetic dipole−dipole interactions between different proton nuclei of the substance under study. The intensity of magnetic dipole−dipole interactions decreases with the distance between interacting particles as $H_{dd} \propto r^{-3}$, so they are long-range interactions. Recall that according to the general classification of potentials, potentials decreasing with distance in three-dimensional space as $H(r) \propto r^{-\alpha}$ at $\alpha \le 3$ are called long-range potentials and at $\alpha > 3$ are called short-range potentials.

Deuterons have spin $I = 1$ and possess a nonzero electric quadrupole moment, so they are capable, in addition to mutual magnetic dipole−dipole interactions, for electric quadrupole interaction with gradients of electric fields created by charges surrounding the deuteron nuclei. The molecules surrounding the deuterium spin are neutral, so the electric field gradient created by them decreases with distance, at least as $H_Q \propto r^{-5}$. Therefore, the quadrupole interactions of deuterium nuclei are short-range and are related mainly to the intramolecular distribution of electron shells on the nearest atoms. The intensity of quadrupole interactions of deuteron spins exceeds the intensity of their mutual magnetic dipole−dipole interactions by a couple of orders of magnitude. Therefore, at the present accuracy of NMR experiments, the contribution

https://doi.org/10.1021/acs.macromol.3c02360
Macromolecules 2024, 57, 3765−3775

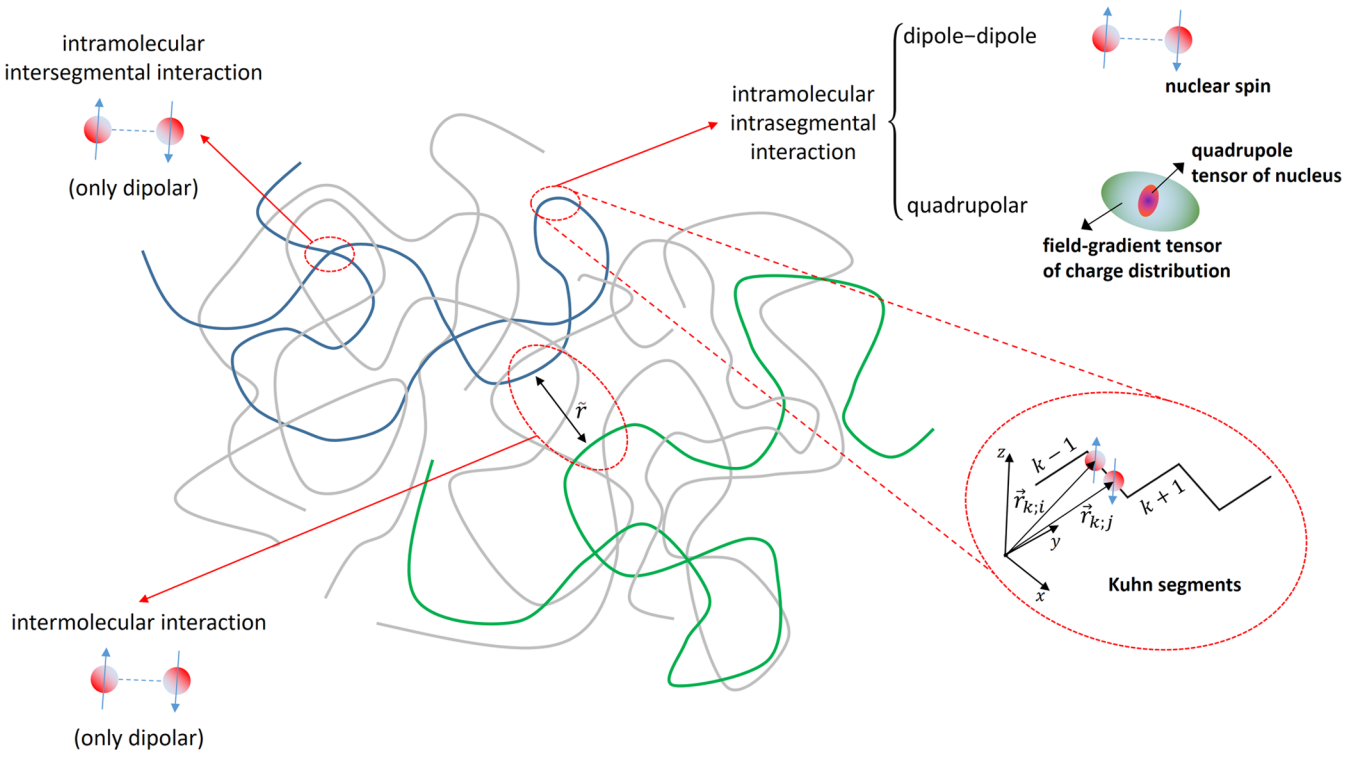

Figure 1. Illustration of different interactions between spins, determining the spin relaxation of the respective nucleus. For proton nuclei, the spin-relaxation results from the magnetic dipole−dipole interaction of different proton nuclei, which can be located on the same (intramolecular) or on different (intermolecular) macromolecules, marked in blue and green. The deuteron relaxation is dominated by the interaction between their quadrupole moments and gradients of electric fields around the nucleus. Due to the short-range nature of the quadrupolar interaction, only intramolecular interactions are of relevance for deuteron relaxation. The enhancement in the red circle shows the position of spins i and j on the kth Kuhn segment, described by their radius-vectors $\vec{r}_{k;i}$ and $\vec{r}_{k;j}$. The relative distance of the two polymer segments on different macromolecules is represented by $\tilde{r}$.

from magnetic dipole−dipole interactions to the deuteron spin-relaxation processes can be neglected compared to the contribution from electric quadrupole interactions. Figure 1 shows an illustration of different spin interactions relevant for the spin relaxation of protons and deuterons in polymer melts.

Note that in the linear approximation by $\hat{H}_{\mathrm{int}}$ (int = dd,Q), the internal interactions discussed above do not give contributions to the relaxation processes at all. If the system under study is anisotropic, the correspondingly averaged linear contributions cause shifts of resonance frequencies, which are usually always many orders of magnitude smaller than the main resonance frequency, ω_0, which allows us to neglect the influence of these shifts on the spin-relaxation rates. The spin relaxation is a second-order effect on the spin−lattice interaction.

The spin−lattice relaxation rate $R_1^{\mathrm{sp}}(\omega) = 1/T_1^{\mathrm{sp}}(\omega)$ where $T_1^{\mathrm{sp}}(\omega)$ is spin−lattice relaxation time, determined from the initial slope of the longitudinal magnetization recovery curve of the sample spin system, is in the most general case represented as the sum of intramolecular and intermolecular contributions

$$R_1^{\mathrm{sp}}(\omega) \equiv R_1^{\mathrm{sp,intra}}(\omega) + R_1^{\mathrm{sp,inter}}(\omega) \equiv \frac{1}{T_1^{\mathrm{sp,intra}}(\omega)} + \frac{1}{T_1^{\mathrm{sp,inter}}(\omega)} \quad (1)$$

where $R_1^{\mathrm{sp,intra}}(\omega) \equiv \frac{1}{T_1^{\mathrm{sp,intra}}(\omega)}$ is the intramolecular contribution and $R_1^{\mathrm{sp,inter}}(\omega) \equiv \frac{1}{T_1^{\mathrm{sp,inter}}(\omega)}$ is the intermolecular contribution, and the index sp = H, D denotes the type of spins investigated, in this paper protons or deuterons.

At resonance frequencies $\omega\tau_s \ll 1$, where τ_s denotes the segmental relaxation time of the macromolecule, due to the large number of intrasegmental internal rotations over times of order $t \sim \omega^{-1}$, there is a partial averaging of the Hamiltonian of intramolecular spin−lattice interactions. The result of this averaging is called the residual part of the Hamiltonian of the spin−lattice interaction. The spatial variables of this residual Hamiltonian appear to depend only on the spatial orientations of the polymer segment on which the intrasegmental spins are localized. They mainly determine the so-called spin−segment coupling constant, also called the order parameter, which is independent of the frequency in the discussed frequency range. Therefore, it is natural to assume that the different spatial components of the Rouse modes in isotropic melts fluctuate independently of each other. In this case, the intramolecular contribution to the initial rate of spin−lattice relaxation of spins located on the same polymer segment has the same structure for protons and deuterons and can be estimated by the method described in, for example, ref 31 and the cited literature

$$R_1^{\mathrm{sp,intra}}(\omega) = \frac{1}{N}\sum_k \int_0^\infty \mathrm{d}t A_k^{\mathrm{sp}} \frac{\langle \vec{b}_k(t)\vec{b}_k(0)\rangle_{\mathrm{eq}}^2}{\langle b_k^4\rangle_{\mathrm{eq}}} \{\cos(\omega t) + 4\cos(2\omega t)\} \quad (2)$$

where A_k^{sp} is the constant that reflects the nature of the spin−lattice interaction of spins located on the polymer segment

https://doi.org/10.1021/acs.macromol.3c02360
Macromolecules 2024, 57, 3765−3775

with number k. Summation is performed over all Kuhn segments of the macromolecule, N is the number of Kuhn segments in one macromolecule, $\vec{b}_k(t)$ is the vector connecting the ends of the Kuhn segment at time t, b_k is the length of the discussed vector, and $\langle\cdots\rangle_{eq}$ denotes averaging with the equilibrium distribution function of the system under study. An introduction and detailed presentation of the most fundamental facts of the quantum mechanics for a spin system is given in ref 32.

For the case of homopolymers, the constant A_k^{sp} and $\langle b_k^4\rangle_{eq}$ do not depend on the polymer segment number k and eq 2 can be rewritten as follows

$$R_1^{sp,intra}(\omega) = \frac{A_n^{sp}}{\langle b_n^4\rangle_{eq}}\frac{1}{N}\sum_k\int_0^\infty dt\langle\vec{b}_k(t)\vec{b}_k(0)\rangle_{eq}^2 \{\cos(\omega t) + 4\cos(2\omega t)\} \quad (3)$$

The common structure of the intrasegmental contributions to the spin−lattice relaxation rate of protons and deuterons is related to the fact that in both cases the spatial coordinate-dependent variables for both magnetic dipole−dipole and electric quadrupole interactions are tensors of the second kind with respect to spatial rotations. In isotropic systems at times $t \gg \tau_s$, the residual part of the corresponding Hamiltonians of spin−lattice interactions will be proportional to the tensors of the second order constructed from the components of the vectors $\vec{b}_k(t)$ (see details for the case of proton relaxation in ref 31), *i.e.*, quadratic in its components b_k^α, where $\alpha = x, y, z$. As already mentioned, spin relaxation is a second-order effect of the spin−lattice interaction. Therefore, the spin-relaxation rate appears to be proportional to the spectral densities of the fourth-order dynamical correlation functions $\langle b_k^\alpha(t)b_k^\beta(t)b_k^\alpha(0)b_k^\beta(0)\rangle_{eq}$, $\alpha \neq \beta$. For isotropic dynamical models, fluctuations of different components of the vector $\vec{b}_k(t)$ can be considered independent of each other, assuming that $\langle b_k^\alpha(t)b_k^\beta(t)b_k^\alpha(0)b_k^\beta(0)\rangle_{eq} \approx 1/9\langle\vec{b}_k(t)\vec{b}_k(0)\rangle_{eq}^2$.

For protons, the constant A_k^H is defined by the following equation

$$A_k^H = \frac{2}{3}\frac{\gamma_H^4\hbar^2 I(I+1)}{\tilde{N}_s}\sum_{i<j}\frac{S_{k;ij}^2}{\langle b_k^4\rangle_{eq}}\left\langle\frac{b_k^2}{r_{k;ij}^3}\right\rangle_{eq}^2 \quad (4)$$

where $S_{k;ij} = \frac{1}{2}\left\langle\frac{3(\vec{e}_{k;ij}\vec{n}_k)^2-1}{r_{k;ij}^3}b_k^2\right\rangle_{eq}\left\langle\frac{b_k^2}{r_{k;ij}^3}\right\rangle_{eq}^{-1}$ —spin−segment coupling constant (order parameter), $\vec{n}_k = \frac{\vec{b}_k}{b_k}$—unit vector oriented along the polymer segment with number k, $\vec{r}_{k;ij}$—radius-vector connecting spins with numbers i and j located on the segment with number k, $\tilde{N}_s$—number of spins located on one segment, $\hbar$—Planck's constant, γ_H —proton gyromagnetic ratio, I—value of spin.

Note that for the case when the fluctuations of the lengths of polymer segments can be neglected and the spins can be considered rigidly bound to the polymer segments, *i.e.*, neglecting the mutual orientation fluctuations of the vectors $\vec{b}_k$ and $\vec{r}_{k;ij}$ arising due to intrasegment internal rotations, the spin−segment interaction parameter (order parameter) $S_{k;ij} = 1$.

For deuterons, the constant A_k^D has the following structure (it can be calculated similar to the discussed proton case using the formalism described in ref 31 and presented in the Supporting Information (SI))

$$A_k^D = \frac{1}{40}\left(\frac{eQ}{\hbar}\right)^2\frac{(2I+3)}{I^2(2I-1)}\langle q_{\tilde{z}\tilde{z}}b_k^2\rangle_{eq}^2 S_{k,Q}^2 \quad (5)$$

where $S_{k,Q} = \frac{1}{2}\frac{\langle(3(\vec{e}_k^{\tilde{z}}\vec{n}_k)^2 - 1 + \eta(1-(\vec{e}_k^{\tilde{z}}\vec{n}_k)^2)((\vec{e}_k^{\tilde{x}}\vec{n}_k)^2 - (\vec{e}_k^{\tilde{y}}\vec{n}_k)^2))q_{\tilde{z}\tilde{z}}b_k^2\rangle_{eq}}{\langle q_{\tilde{z}\tilde{z}}b_k^2\rangle_{eq}}$ is the spin−segment coupling constant (order parameter) of the quadrupole electric interaction of the deuteron located on the polymer segment with number k, e is the elementary electric charge (electron charge), eQ is the quadrupole moment of deuterium, $\eta = \frac{q_{\tilde{x}\tilde{x}} - q_{\tilde{y}\tilde{y}}}{q_{\tilde{z}\tilde{z}}}$ is the so-called asymmetry parameter of the electric field gradient, $q_{\tilde{x}\tilde{x}}$, $q_{\tilde{y}\tilde{y}}$, and $q_{\tilde{z}\tilde{z}}$ are principal values of the tensor of the electric field gradient acting on the deuterium nucleus located on the polymer segment with number k, $\vec{e}_k^{\tilde{x}}$, $\vec{e}_k^{\tilde{y}}$, and $\vec{e}_k^{\tilde{z}}$ are unit vectors of the direction of the principal axes $\tilde{x}$, $\tilde{y}$, $\tilde{z}$ of the tensor of the discussed electric field gradient, and $I = 1$ for deuterons.

Note that in order to simplify the mathematical formulas, eq 5 is written for the case when on each polymer segment the electric quadrupole fields are the same for all spins located on this segment. Generalization to a more general case does not affect the structure of eq 3, but leads to only a more cumbersome, although obvious, equation for the constant A_k^D (see SI), the exact value of which is not essential for this paper. For the limiting case when the principal direction of the electric field gradient tensor is rigidly related to the direction of the vector connecting the ends of the polymer segment, *i.e.*, $\vec{e}_k^{\tilde{z}} = \vec{n}_k$, $S_{k,Q} = 1$ as in the case of protons discussed above.

In the intermediate time limit $\tau_s \ll t \ll \tau_1$, where τ_1 is the terminal relaxation time characterizing relaxation of the whole chain, the autocorrelation function of the tangent vector $\langle\vec{b}_k(t)\vec{b}_k(0)\rangle_{eq}$ is related to the mean-squared displacement of the segments $\langle r_k^2(t)\rangle_{eq}$ as[15−17]

$$\langle r_k^2(t)\rangle_{eq}\langle\vec{b}_k(t)\vec{b}_k(0)\rangle_{eq} = \beta\frac{b^4}{\pi} \quad (6)$$

where β is a numerical coefficient of order 1, depending on the details of the dynamical model.

If we assume that the mean-squared displacement of the polymer segments depends on time by a power law with an exponent α, *i.e.*, $\langle r_k^2(t)\rangle_{eq} \propto t^\alpha$, based on eqs 1−6, we obtain the following dependence of the intramolecular contribution on the resonance frequency

$$R_1^{sp,intra}(\omega) \propto \int_0^\infty \frac{\cos(\omega t) + 4\cos(2\omega t)}{\langle r_k^2(t)\rangle_{eq}^2}dt \propto \frac{\pi(1+2^{1+2\alpha})}{2\cos(\alpha\pi)\Gamma\left(\frac{\alpha}{2}\right)}\omega^{2\alpha-1} \propto \omega^{2\alpha-1} \quad (7)$$

The intermolecular contribution to the proton spin−lattice relaxation rate has a different frequency dependence. The following equation was obtained for the intermolecular contribution to the spin−lattice relaxation rate for isotropic systems[29,30,33]

$$R_1^{H,inter}(\omega) = \frac{16}{15}\sqrt{\frac{3\pi}{2}}\gamma_H^4\hbar^2 I(I+1)n_H \int_0^\infty \frac{\cos(\omega t) + 4\cos(2\omega t)}{(\sigma^* + \langle\tilde{r}^2(t)\rangle_{eq}^{1/2})^3}dt \quad (8)$$

https://doi.org/10.1021/acs.macromol.3c02360
Macromolecules 2024, 57, 3765−3775

where n_H is the concentration of protons in the system, $\sigma^* \propto (b^2\rho_s)^{-1}$ is the microscopic quantity characterizing the spatial separation of closest segments from different macromolecules, ρ_s is the concentration of polymer segments, $n_H = \tilde{N}_s\rho_s$, $\langle \tilde{r}^2(t)\rangle_{eq}$ is the relative mean-squared displacement of two polymer segments from different macromolecules during the time interval t.

If we assume that $\langle \tilde{r}_k^2(t)\rangle_{eq} = 2\langle r_k^2(t)\rangle_{eq}$, we obtain for times $\tau_s \ll t$ the following frequency dependence for the intermolecular contribution to the proton spin−lattice relaxation rate

$$R_1^{H,inter}(\omega) \propto \int_0^\infty \frac{\cos(\omega t) + 4\cos(2\omega t)}{\langle r_k^2(t)\rangle_{eq}^{3/2}} dt \propto \frac{\pi(1 + 2^{1+3\alpha/2})}{2\cos(\alpha\pi)\Gamma\left(\frac{\alpha}{2}\right)}\omega^{3\alpha/2-1} \propto \omega^{3\alpha/2-1} \quad (9)$$

Comparing relations (7) and (9), it is easy to see that at sufficiently low resonance frequencies, the intermolecular contribution to the proton spin−lattice relaxation rate will dominate over the intramolecular contribution (see a more detailed discussion in ref 33). Furthermore, the difference between eqs 7 and 8−9 is the following: eq 7 is an approximation for eq 2, which contains contributions only from internal dynamical modes and not those from the center of mass diffusion. As was mentioned above, it is valid for the time interval $\tau_s \ll t \ll \tau_1$; eq 9 contains contributions from all dynamical modes including the center of mass diffusion, and it is valid within the more extensive time interval $\tau_s \ll t$.

In the case of deuteron spins, in principle, there are also contributions from intermolecular magnetic dipole−dipole interactions. For them, the relation (8), in which the gyromagnetic ratio of protons should be replaced by the gyromagnetic ratio of deuterons, is applicable in good approximation with the value of spin $I = 1$. However, the corresponding contribution is negligibly small compared to the contribution from electric quadrupole interactions of intramolecular nature. Therefore, at the existing accuracy of experiments, the discussed contribution to the spin−lattice relaxation rate of deuterons is neglected.

The intermolecular contribution to the proton spin−lattice relaxation rate, as seen in eq 8, depends on the concentration of protons in the system n_H, while the intramolecular contribution from protons located on the same Kuhn segment of the macromolecule is independent from n_H. This circumstance allows diluting protonated macromolecules with their deuterated analogues having the same number of Kuhn segments in the macromolecule, changing the ratio between intramolecular and intermolecular contributions to the spin−lattice relaxation rate in formula 1 (see details in ref 34) to experimentally separate these contributions.

Equations 2 and 3 imply averaging over all Kuhn segments of the macromolecule, which for the case of linear macromolecules is equivalent to neglecting end effects, which possess, as shown in refs 35−37, a frequency character, *i.e.*, dependent on the observation time. For the case of proton spin−lattice relaxation, this is quite an acceptable approximation since in polymer melts the spin−lattice relaxation times are much longer than the characteristic times of interspin flip−flop transitions leading to the formation of spin temperature in multispin systems, averaging the rates of proton spin−lattice relaxation. For spin−spin relaxation as measured, for example, by the Hahn echo method, such an approximation is obviously not possible since the times of interspin transitions are larger than the characteristic times of spin−spin relaxation. This is especially characteristic, as shown in refs 35−37, for the case of spin−spin relaxation of deuteron nuclei in melts of linear macromolecules. The dynamic heterogeneity of different segments of linear macromolecules generated by end effects leads to a strong nonexponential attenuation of the Hahn echo signals.

Spin−spin relaxation in the melts of ring macromolecules, under the assumption that during the spin-relaxation time the segments of macromolecules have time to translate over distances of the order of the linear sizes of the rings, i.e., $R_g \propto bN^{1/3}$, should not lead to nonexponentiality of the spin echo signal decays, since all segments during the period of time under discussion find themselves in equivalent positions relative to the center of mass.

EXPERIMENTS

Linear PEO (hL) of different molar masses were purchased from Polymer Standards Service GmbH (Mainz, Germany), while the PEO rings (hR) were synthesized by Forschungszentrum Jülich GmbH (Jülich, Germany). The procedure for the synthesis and characterization of the PEO rings is presented elsewhere.[10,12,38] The synthesis and characterization of ring polymers with molecular weights up to 20 kg/mol are described in detail in ref 38. Synthesis and characterization of large molecular weight rings is presented in the Supporting Information to refs 10 and 12. Perdeuterated variants (dL and dR) of similar molar masses were purchased or synthesized by the same institutions. In the case of the ring samples, the perdeuterated variants were used to prepare an isotope blend (R) containing 90 wt % perdeuterated and 10 wt % proton-bearing macromolecules of similar molar mass. The blends were obtained by dissolving the corresponding amounts of polymers in chloroform and subsequent freeze-drying. The molar characteristics of the PEO rings and chains are summarized in Tables 1 and 2. The samples were placed in

Table 1. Molecular Weights of Polymer Rings Used in This Study M_n, Molecular Weight Distribution M_w/M_n, the Number of Entanglements per Macromolecule $Z_e = M_n/M_e$, with the PEO Entanglement Molar Weight M_e = 1980 Da, and R_g—Gyration Radius Determined by SANS[10−12,38,39]

sample	M_n (Da)	M_w/M_n	Z_e	R_g (Å)
hR5	5470	1.01	3	15.6
dR5	5280	1.03	3	
hR20	20,100	1.03	10	27.8
hR40	44,000	1.01	22	38.5
dR40	38,600	1.01	19	35.4
hR100	87,300	1.01	44	49.2
dR100	96,000	1.01	48	49.4

3 mm (Hahn Echo experiment) or 5 mm (FFC experiment) NMR tubes and either covered with argon and flame-sealed (linear PEO in 3 mm tubes) or sealed under vacuum conditions.

Longitudinal relaxation dispersion measurements $T_1(\nu)$ were carried out by using a fast field cycling (FFC) relaxometer (Spinmaster FFC2000, Stelar, Mede, Italy) at about 20 different magnetic field strengths between 0.1 mT and 0.5 T. The typical number of scans was 2−4 and a polarization field

https://doi.org/10.1021/acs.macromol.3c02360
Macromolecules 2024, 57, 3765−3775

Table 2. Molecular Weights of Linear Polymers Used in This Study, Molecular Weight Distribution, and the Number of Entanglements per Chain $Z_e = M_n/M_e$

sample	M_n (Da)	M_w/M_n	Z_e
hL3	2800	1.09	<2
dL3	3080	1.11	<2
hL6	6170	1.06	3
hL10	8920	1.12	5
hL18	14,900	1.20	8
hL30	26,400	1.10	13
dL33	31,300	1.10	16
hL41	31,700	1.30	16
hL95	81,900	1.16	41
hL180	148,000	1.22	75
hL220	197,000	1.12	99

of 0.47 T was used. For detection, a single $\pi/2$ pulse is used, and the probe was tuned to 16.7 MHz with the detection field set at the corresponding field strength of 0.392 T.

The transverse relaxation decays were measured with a Bruker Avance III spectrometer equipped with a solid-state probe head operating at a ^{1}H resonance frequency of 300 MHz by using a Hahn echo pulse sequence $(\pi/2 - \tau - \pi - \tau)$. The duration of π-pulse t_π, typically 10 μs, was twice the length of the $\pi/2$ pulse. A recycle delay of 5 T_1 was applied between the repetitions of the pulse sequence to allow for complete longitudinal relaxation.

All measurements were carried out in the molten state of the samples at different temperatures (see figures) between 343 and 373 K.

RESULTS AND DISCUSSION

We begin our discussion with Figure 2, which shows the normalized Hahn echo decay curves for melts of linear and ring macromolecules. The time axis is measured in spin−spin relaxation time units, T_2^{eff}, defined as $A_{\text{norm}}(T_2^{\text{eff}}) = e^{-1}$ and whose absolute values can be found in the Supporting Information (SI).

In melts of linear macromolecules (Figure 2a,c), the normalized echo decays are strongly nonexponential. Moreover, the nonexponentiality increases with increasing molecular weight. This is a consequence of the dynamic heterogeneity of the linear melt induced by the end segments whose influence on the dynamics of other segments is not trivial and has a frequency nature (see refs 35,36 for a detailed discussion). At first glance, it seems that the observed increase in the degree of nonexponentiality of the echo decay with increasing molecular weight of macromolecules cannot be due to the dynamic heterogeneity of macromolecule segments caused by the presence of end segments since their contribution to the observed echo signal should seem to decrease with increasing

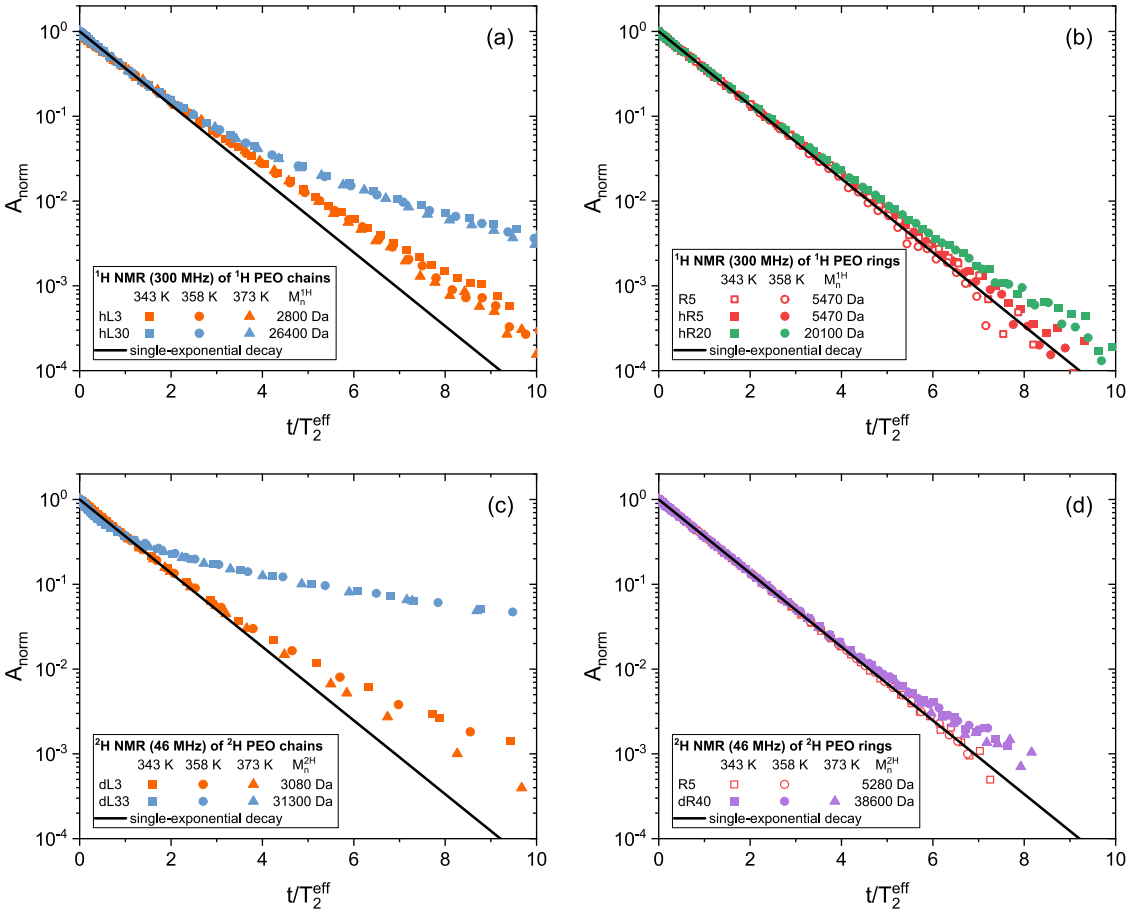

Figure 2. Semilogarithmic representation of ^{1}H (a,b) and ^{2}H (c,d) Hahn Echo decay at 7.05 T in melts of PEO chains (a, c) and rings (b, d) in bulk and a 10/90 ^{1}H/^{2}H blend with corresponding molar masses. The x-axis is normalized to T_2^{eff}. The black line serves as a guide for the eye and represents a single-exponential decay according to $A_{\text{norm}} = \exp(-t/T_2^{\text{eff}})$. $A_{\text{norm}}(t)$ is the normalized area below the PEO peak in the spectrum, which is obtained by Fourier transform of the signal resulting from the Hahn echo pulse sequence at time $t = 2\tau + t_\pi$.

https://doi.org/10.1021/acs.macromol.3c02360
Macromolecules 2024, 57, 3765−3775

number of Kuhn segments as N^{-1}. However, as it follows from the works mentioned above,[35,36] the situation is not so straightforward. The point is that the dynamic heterogeneity caused by the presence of end segments of the macromolecule in the geometrical (topological) sense turned out to have a frequency character; *i.e.*, it depends on the observation time. As the observation time increases, the number of segments whose mobility is higher than that of the central segments increases symmetrically with respect to both ends of the macromolecule. The latter is inherent in all dynamic polymer models, although to different degrees. This can be illustrated most clearly in terms of the classical reptation model. In this case, the lifetime of a macromolecule segment in the initial tube along which the macromolecule makes reptation movements is a monotonically increasing function of its curvilinear distance to the nearest end of the primitive chain. When the Redfield limit (the limit of fast motions) is satisfied, *i.e.*, $T_2 > \tau_1$ where τ_1 is the terminal relaxation time of macromolecules, the spins located on the same primitive segment relax exponentially and the corresponding spin−spin relaxation times appear to be functions of the numbers of primitive segments. As the molecular mass of macromolecules increases, the number of primitive tube segments also increases, so that the measured total decay of the Hahn echo signal turns out to be the sum of an increasing number of individual exponential contributions; *i.e.*, the degree of nonexponentiality increases. At large molecular masses, when the Redfield limit is violated, the situation qualitatively remains the same, with an additional complication due to the fact that the relaxation decays of individual spins are no longer exponential.[36] Note also that this expected decrease in the nonexponentiality of the Hahn echo decay with increasing molecular mass N should occur under the condition that the observation time t is fixed and the molecular mass N increases. The experiments discussed above were carried out without fixing the observation time. The degree of entanglement of polymer melts, which increases with molecular weight, leads to a decrease in the spin−spin relaxation time with increasing molecular weight more rapidly than the logarithmic decrease predicted by the Rouse model.

It is possible to see that the dynamic heterogeneity of the investigated deuterated samples is significantly stronger than that of the protonated samples. The latter is due to the fact that in the case of deuterated samples, spin relaxation is determined mainly only by fluctuations of the electric field gradient created by intrasegmental atoms. The spin relaxation of protons is determined by thermal fluctuations of magnetic dipole−dipole interactions, which have both intramolecular and intermolecular contributions. Intermolecular contributions to spin relaxation are associated with all segments of neighboring macromolecules, located both at the end and in the middle. Therefore, their contributions partially diminish the effect of the dynamic heterogeneity in melts of linear macromolecules on proton spin relaxation compared to that of deuteron spin relaxation.

In melts of ring macromolecules, we see, within experimental errors, predominantly exponential decays of the normalized Hahn echoes, in other words, the absence of dynamic heterogeneity of ring macromolecules. This effect, in our opinion, is not as obvious as it might seem at first glance. Ring macromolecules in melts have dense, globular conformations. Therefore, the absence of end segments alone is not sufficient for the elimination of dynamic heterogeneity. An additional necessary condition for the dynamic homogeneity of segments included in the globule structure is their possibility of being in all possible positions relative to the center of mass of the globule during the experiment. It is this fact that is demonstrated by the decays of the normalized Hahn echoes presented in Figure 2.

The globular state of the ring macromolecule in a melt is a highly fluctuating state. It should be noted here that in this respect the globular state of cyclic macromolecules in melts qualitatively differs from the globular state of biological proteins whose constituent elements make relatively small displacements relative to sufficiently fixed positions in the system of the globule center of mass. The dynamics and structure of the former have been intensively studied by the so-called T_2 dispersion method.[40−42]

Let us continue with the discussion of the frequency dispersion of the proton spin−lattice relaxation times, which is shown in Figure 3 for melts of mixed deuterated and

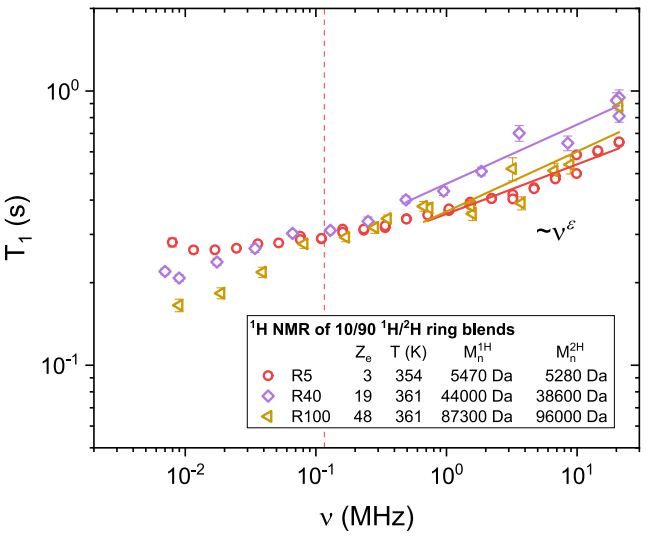

Figure 3. Proton spin−lattice relaxation dispersion measured by FFC in blends of 10 wt % proton-bearing (hR5, hR40, hR100) and 90 wt % deuterated (dR5, dR40, dR100) rings of similar molar masses. The solid lines represent a power law obtained from a linear fit without error weighting in the indicated range. For R40 and R100, a similar exponent $\varepsilon \approx 0.22$ is observed, while R5 exhibits a slightly lower exponent ($\varepsilon \approx 0.18$, see Table 3) The exponent 0.22 corresponds to $\langle r_n^2(t)\rangle \propto t^{0.39} \approx t^{2/5}$. The dashed red line marks the terminal relaxation time of linear PEO with $Z_e \approx 3$, *i.e.*, $M_n = 5940$ *Da*.

protonated ring macromolecules with molecular weights of approximately 5000, 40,000, and 100,000 Da (see Table 1). The frequency range of the experiments covers the interval 8×10^3 to 2×10^7 Hz, which corresponds to the time interval 8×10^{-9} to 2×10^{-5} s. Note that quasielastic neutron scattering experiments cover the time interval of 10^{-12} to 10^{-6} s. Thus, there is a certain overlap region of the two discussed experiments.

For the large molecular weight mixtures (10 wt % protonated and 90 wt % deuterated polymers) R100 ($Z_e \approx 44$) and R40 ($Z_e \approx 22$), a proton frequency, $\nu = \omega/2\pi$, dispersion of the spin−lattice relaxation time constant $T_1(\nu) = \frac{1}{R_1(\nu)}$ with a slope of $\varepsilon = 0.22 \pm 0.04$ is observed above about 0.5 MHZ (see Table 3 for individual slopes), characterizing $T_1(\nu)$ toward the high-frequency end of the investigated frequency range. Since the blends consist of only 10 wt %

https://doi.org/10.1021/acs.macromol.3c02360
Macromolecules 2024, 57, 3765−3775

Table 3. Terminal Relaxation Times τ_1 and Slopes ε and θ of the Proton-Bearing Ring (hR) and Linear (hL) Samples as well as the Isotope Mixtures (R) of 10 wt % Proton-Bearing and 90 wt % Deuterated Rings[a]

figure	sample	τ_1 (s)	slope ε	slope θ
Figure 3	R5	1.38×10^{-6}	0.181 ± 0.011	
	R40	3.50×10^{-4}	0.216 ± 0.024	
	R100	5.64×10^{-3}	0.219 ± 0.046	
Figure 5a	hR5	1.38×10^{-6}	0.216 ± 0.009	
	hR20	5.10×10^{-5}	0.213 ± 0.004	0.424 ± 0.010
	hR100	4.35×10^{-3}	0.215 ± 0.006	0.461 ± 0.038
Figure 5b	hL6	1.38×10^{-6}	0.207 ± 0.018	
	hL10	6.38×10^{-6}	0.246 ± 0.012	
	hL18	2.61×10^{-5}	0.234 ± 0.021	0.305 ± 0.009
	hL41	2.09×10^{-4}	0.226 ± 0.005	0.340 ± 0.011
	hL95	3.52×10^{-3}	0.237 ± 0.025	0.336 ± 0.010
	hL180	2.15×10^{-2}	0.235 ± 0.014	0.343 ± 0.013
	hL220	4.95×10^{-2}	0.249 ± 0.017	0.354 ± 0.010

[a]The slopes ε and θ are obtained from a linear fit without error weighting, performed with OriginPro 2022, of the FFC data as shown in Figures 3 and 5, *i.e.*, toward the high (ε) and low (θ) frequency limit of the investigated frequency range. The corresponding terminal relaxation times for linear PEO are calculated according to $\tau_1 = 3\tau_s N_e^2 Z_e^3$ with the average number of Kuhn segments between two entanglements $N_e = M_e/m_k$ and the number of entanglements per chain $Z_e = M_n/M_e$, using m_k = 137 Da[18] as the molar mass of a Kuhn segment and Z_e from Tables 1 and 2. In the case of the isotope mixtures, Z_e of the perdeuterated samples were used for the calculation. The segmental relaxation time is estimated as $\tau_s = \frac{1}{9\pi^2}\frac{b^2 N_e}{D_{cm} N_{ref}{}^2} \cong 8.14 \times 10^{-11}$s by using the Kuhn length b = 11 Å,[18] the center of mass diffusion for the reference molar mass $D_{cm}(M_{ref}$ = 12,300 g/mol) = 3×10^{-13} m^2/s,[44] and $N_{ref} = M_{ref}/m_k$, the number of Kuhn segments in the reference macromolecule.

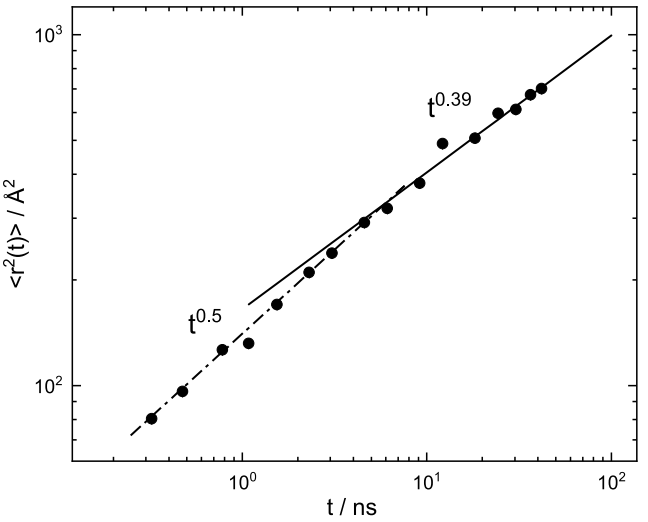

Figure 4. Segmental mean-squared displacement derived from the incoherent spectra measured by the neutron spin echo for the rings hR100 (M_n = 87,300 *Da*).[12] The lines display the limiting power laws for Rouse motion $t^{0.5}$ and an empirical power law $t^{0.39}$.

proton-bearing macromolecules, the intermolecular contributions to the fluctuations of the magnetic dipole−dipole interactions are negligible. Therefore, in accordance with eq 7, the mean-squared displacement of the segments $\langle r_n^2(t)\rangle \propto t^{\alpha}$ is connected to the exponent of the spin−lattice relaxation frequency dispersion by $R_1^{intra}(\omega) \propto \omega^{2\alpha-1} = \omega^{-0.22\pm0.04}$, *i.e.*, $\alpha \approx$ 0.39. A power law with this exponent shows reasonable agreement with the neutron scattering data presented in Figure 4 at times larger than $t > 7 \times 10^{-9}$ s.

In the melts of the small rings R5 ($Z_e \approx 3$), the observed dispersion of the proton spin−lattice relaxation decreases toward low frequencies and approaches a plateau. This is due to the fact that frequency dispersion can be observed only at sufficiently high frequencies $\tau_1^{int} \gg 1$, where τ_1^{int} is the terminal time of internal rotational modes of the macromolecule for which thermal fluctuations induce intramolecular spin-relaxation processes. A comparison with the calculated terminal relaxation time for linear PEO with $Z_e \approx 3$ (see Table 3) shows reasonable agreement with the onset of the plateau in Figure 3.

Figure 5 shows the frequency dispersions of the proton spin−lattice relaxation in melts of ring (5a) and linear macromolecules (5b). In contrast to the blends in Figure 3, the macromolecules are solely proton-bearing; therefore, both contributions to the fluctuations of the magnetic dipole−dipole interactions, intra- and intermolecular, must be considered (see Figure 1). With increasing time, e.g., at lower frequency, as seen from our measurements, the intermolecular contributions become more important. Thus, at high frequencies there is a dominance of intramolecular contributions, while at lower frequencies intermolecular contributions dominate (see details in refs 28−30 and the literature cited therein).

The averaged power-law exponents for all three molecular weights, $\langle\varepsilon\rangle$ = 0.215 ± 0.006 in the region above 1 MHz (hR5) and 0.1 MHz (hR20 and hR100), *i.e.*, toward the high frequency, are found to be equivalent to the values found for the diluted samples presented in Figure 3 ($\langle\varepsilon\rangle$ = 0.205 ± 0.027, see also Table 3 for individual slopes). This allows us to estimate the exponent of the frequency dependence of the intermolecular contribution of the spin−lattice relaxation rate based on the exponent of the mean-squared displacement α = 0.39, extracted earlier from Figure 3. According to eq 9, $R_1^{inter}(\omega) \propto \omega^{3\alpha/2-1} = \omega^{-0.415}$, an exponent of about 0.415 is expected for the spin−lattice relaxation time frequency dispersion. The obtained result is quite close to the experimentally observed averaged power law of $\langle\theta\rangle$ = 0.44 ± 0.02 (see Table 3) found for the rings of different molecular weights at the low-frequency limit in Figure 5a. It also indicates that despite the globular conformation of ring macromolecules, their mutual penetration is quite strong. The latter is in qualitative agreement with computer simulation data[14] where it was noted that the concentration of neighboring ring macromolecules in the center of mass of the globule reaches approximately 60%. Note that in the melt of linear macromolecules, the above concentration reaches 100% with precision to values of the order of $N^{-1/2}$.[17−20] Such a decrease in the concentration of segments of neighboring macromolecules in ring melts compared with their linear counterparts naturally reduces the contribution of intermolecular magnetic dipole−dipole interactions compared to intramolecular ones.

Comparing Figure 5a with b, we see that the crossover to a larger exponent of the spin−lattice relaxation dispersion in the melt of ring macromolecules occurs at frequencies of the order of magnitude lower compared to the melt of linear macromolecules. The mean-squared displacement of the ring molecules related to this crossover time estimated based on the available diffusion coefficients[12] corresponds to 1.5−2 Å

https://doi.org/10.1021/acs.macromol.3c02360
Macromolecules 2024, 57, 3765−3775

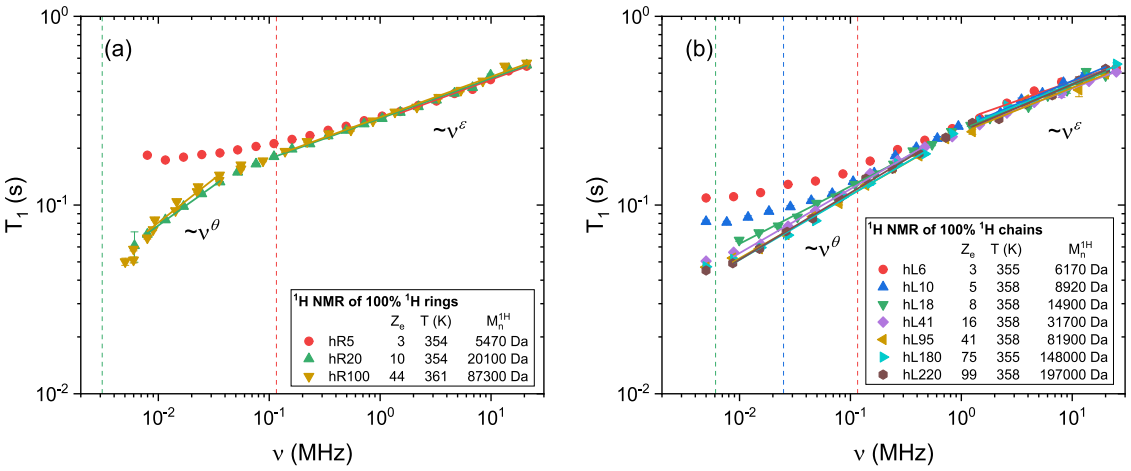

Figure 5. Proton spin−lattice relaxation dispersion for rings hR5, hR40, and hR100 (a) and linear analogues (b) (see Table 2). The corresponding power laws are shown by solid lines and were obtained from linear fits without error weighting in the indicated range. The individual exponents ε and θ can be found in Table 3. The dashed lines mark the terminal relaxation time calculated for linear PEO with the corresponding Z_e indicating the expected transition to the plateau values.

for rings that are smaller than the size of the ring itself. This is associated with the abovementioned decrease in the concentration of segments of neighboring macromolecules in the center of mass of the globule. Also note that in the case of melts of linear macromolecules, the contribution of intermolecular magnetic dipole−dipole interactions is important already starting from the highest experimental frequencies.[37] The transition from the observed exponent of about 0.25 at high frequencies to an exponent of about 0.35 at low frequencies is associated with an increased influence of entanglement on the segmental dynamics.[29,30,33]

Based on rough estimations, we calculate the size of ring macromolecules as a function of different conformations.

For a freely jointed ideal ring, the radius of gyration is[1]

$$\tilde{R}_g^{fr} = \sqrt{\frac{Nb^2}{12}} \tag{10}$$

For a ring densely packed into a spherically symmetric globule, the radius of this globule is equal to

$$R^{sf} = \left[\frac{3}{4\pi}\frac{m_p}{\rho}M\right]^{1/3} \approx 0.72 \times M^{1/3}\text{Å} \tag{11}$$

where M is the molecular weight in Daltons, $\rho(353\ K) \approx (1.06\cdots1.08)$ g/cm^3[45] is the density of the PEO melt, m_p is the proton mass. Note that the gyration radius of such a sphere is equal to $\tilde{R}_g^{sf} = \sqrt{\frac{3}{5}}R^{sf}$. Using b = 11 Å,[18] the size of the large molar mass rings, hR100 (M_n = 87,300 Da, $N = M_n/m_k \approx 637$) and dR100 (M_n = 96,000 Da, $N \approx 701$), can be estimated as $R^{sf} \approx 32$ Å, $\tilde{R}_g^{sf} \approx 25$ Å, and $\tilde{R}_g^{fr} \approx 82$ Å. The small angle neutron scattering (SANS) experiment finds for the discussed molecular mass of ring macromolecules $R_g^{exp} \approx 49$ Å.[11,12] Thus, the real size of the globule is significantly smaller compared to a random freely joint ideal ring but significantly larger than the globular structure corresponding to dense packing. As it follows from the experimental data of refs 37,43 in linear PEO melts with high molecular masses at a temperature T = 363 K on the time interval 10^{-8} to 10^{-4} s, the square root of the mean-squared segmental displacement in this time interval $\langle r_n^2(t)\rangle^{1/2} \approx 15-45$ Å. Note that in the ring melts, the displacements on the indicated time interval are at least of the same magnitude or larger than these values. The latter directly follows from the fact that spin-relaxation times of protons of cyclic macromolecules under otherwise equal conditions, molecular masses, temperatures, and resonance frequencies are longer than spin-relaxation times of linear macromolecules, which indicates their greater mobility in the range of molecular masses and frequencies studied. Note also that the latter qualitatively correlates with simulations.[7,8] In this case, the displacements in the low-frequency interval corresponding to times of order $10^{-5}-10^{-4}$ s are comparable to or larger than the gyration radius of the hR100 ring. Nevertheless, the experimental data obtained by us do not indicate a normal diffusion regime. Qualitatively similar anomalous behavior was also observed in computer simulations[8,15] and by neutron scattering (NSE).[11,12]

CONCLUSIONS

In this study, NMR echo and field-dependent relaxation time measurements were carried out for the first time on ring-shaped polymers, in this case poly(ethylene oxide) rings with narrow molecular weight distributions. Experiments were carried out on bulk protonated melts and in 10:90 protonated mixtures in deuterated chains, the latter with the purpose of suppressing intermolecular contributions to relaxation. Echo experiments showed, in stark contrast to the results from linear chain molecules, monoexponential behavior, which is indicative to the absence of dynamic heterogeneities, while linear chains possess strong heterogeneity that becomes more pronounced with increasing molecular weight. Echo experiments further confirm the absence of chain ends in the investigated ring samples. The frequency-dependent relaxation study of ^{1}H nuclei shows identical behavior for those diluted with deuterated ring analogues and fully protonated rings above about 1 MHz, suggesting the dominance of intramolecular contributions in this frequency range. The power law can then be translated into a root mean-squared displacement dependence proportional to $t^{0.39}$, a subdiffusive behavior that is in excellent agreement with findings from neutron scattering that addresses a higher-frequency window. With this relation, the low-frequency (intermolecular)

https://doi.org/10.1021/acs.macromol.3c02360
Macromolecules 2024, 57, 3765−3775

relaxation dispersion was also predicted and found to describe the NMR experimental results perfectly. These results support a self-consistent description of PEO ring dynamics over a considerable frequency range and explain the NMR response of the ^{1}H nuclei by a sum of intra- and intermolecular contributions originating from the same dynamics of the molecules, despite the absence of a reptation mechanism. We assume the interchain interaction between the ring macromolecules detected using the NMR relaxation techniques can be described in terms of specific interaction potential and requires further investigations.

Despite these findings for rings of intermediate size, we note that the dynamics of ring macromolecule melts is, in our opinion, still very far from a full understanding. The most fundamental and intriguing question is related to the possibility of dynamic localization of ring macromolecules in melts at sufficiently large molecular masses,[6,15] leading to an exponentially fast decrease in the self-diffusion coefficient of ring macromolecules and the presence of a viscoelastic plateau. Note that the presence of such localization should be reflected in the peculiarities of spin relaxation. While theoretical predictions exist for asymptotically large rings, a test of these predictions will require applying the very same methods to newly synthesized samples with larger M_w. It can be assumed that with progress in the synthesis of well-characterized ring macromolecules of large molecular masses, this circumstance will be reliably resolved experimentally.

■ ASSOCIATED CONTENT

Data Availability Statement

The data that support the findings of this study are available from the authors upon reasonable request.

Supporting Information

The Supporting Information is available free of charge at https://pubs.acs.org/doi/10.1021/acs.macromol.3c02360.

Calculation of effective spin−spin relaxation T_2^{eff} and derivation of spin−lattice and spin−spin relaxation rates (PDF)

■ AUTHOR INFORMATION

Corresponding Authors

Siegfried Stapf − *Technische Physik II/Polymerphysik, Technische Universität Ilmenau, D-98684 Ilmenau, Germany;* orcid.org/0000-0001-5191-0416; Phone: +49 3677 693671; Email: Siegfried.stapf@tu-ilmenau.de

Margarita Kruteva − *Jülich Centre for Neutron Science (JCNS-1) and Institute for Biological Information Processing (IBI-8), Forschungszentrum Jülich GmbH, 52428 Jülich, Germany;* orcid.org/0000-0002-7686-0934; Email: m.kruteva@fz-juelich.de

Authors

Kevin Lindt − *Technische Physik II/Polymerphysik, Technische Universität Ilmenau, D-98684 Ilmenau, Germany*

Nail Fatkullin − *Technische Physik II/Polymerphysik, Technische Universität Ilmenau, D-98684 Ilmenau, Germany*

Carlos Mattea − *Technische Physik II/Polymerphysik, Technische Universität Ilmenau, D-98684 Ilmenau, Germany;* orcid.org/0000-0002-3051-928X

Jürgen Allgaier − *Jülich Centre for Neutron Science (JCNS-1) and Institute for Biological Information Processing (IBI-8), Forschungszentrum Jülich GmbH, 52428 Jülich, Germany;* orcid.org/0000-0002-9276-597X

Complete contact information is available at: https://pubs.acs.org/10.1021/acs.macromol.3c02360

Notes

The authors declare no competing financial interest.

■ ACKNOWLEDGMENTS

K.L., N.F., C.M., and S.S. acknowledge financial support from the Deutsche Forschungsgemeinschaft under Research Grant No. STA 511/13-2. The authors thank Artur Lozovoi for collecting part of the FFC data for linear PEO presented in Figure 5b.

■ REFERENCES

(1) Yamakawa, H. *Modern Theory of Polymer Solutions, Electronic ed.*; Harper & Row, 1971, p 434.

(2) Rubinstein, M. Dynamics of Ring Polymers in the Presence of Fixed Obstacles. *Phys. Rev. Lett.* **1986**, *57*, 3023−3026.

(3) Kruteva, M.; Allgaier, J.; Richter, D. Topology Matters: Conformation and Microscopic Dynamics of Ring Polymers. *Macromolecules* **2023**, *56*, 7203−7229.

(4) Ge, T.; Panyukov, S.; Rubinstein, M. Self-Similar Conformations and Dynamics in Entangled Melts and Solutions of Nonconcatenated Ring Polymers. *Macromolecules* **2016**, *49*, 708−722.

(5) Dell, Z. E.; Schweizer, K. S. Intermolecular Structural Correlations in Model Globular and Unconcatenated Ring Polymer Liquids. *Soft Matter* **2018**, *14*, 9132−9142.

(6) Mei, B.; Dell, Z. E.; Schweizer, K. S. Microscopic Theory of Long-Time Center-of-Mass Self-Diffusion and Anomalous Transport in Ring Polymer Liquids. *Macromolecules* **2020**, *53*, 10431−10445.

(7) Halverson, J. D.; Lee, W. B.; Grest, G. S.; Grosberg, A. Y.; Kremer, K. Molecular dynamics simulation study of nonconcatenated ring polymers in a melt. I. Statics. *J. Chem. Phys.* **2011**, *134*, No. 204904.

(8) Halverson, J. D.; Lee, W. B.; Grest, G. S.; Grosberg, A. Y.; Kremer, K. Molecular dynamics simulation study of nonconcatenated ring polymers in a melt. II. Dynamics. *J. Chem. Phys.* **2011**, *134*, No. 204905.

(9) Tsalikis, D. G.; Mavrantzas, V. G.; Vlassopoulos, D. Analysis of Slow Modes in Ring Polymers: Threading of Rings Controls Long-Time Relaxation. *ACS Macro Lett.* **2016**, *5*, 755−760.

(10) Kruteva, M.; Allgaier, J.; Monkenbusch, M.; Porcar, L.; Richter, D. Self-similar Polymer Ring Conformations Based on Elementary Loops: A Direct Observation by SANS. *ACS Macro Lett.* **2020**, *9*, 507−511.

(11) Kruteva, M.; Monkenbusch, M.; Allgaier, J.; Holderer, O.; Pasini, S.; Hoffman, I.; Richter, D. Self-Similar Dynamics of Large Polymer Rings: A Neutron Spin Echo Study. *Phys. Rev. Lett.* **2020**, *125*, No. 238004.

(12) Kruteva, M.; Allgaier, J.; Monkenbusch, M.; Hoffmann, I.; Richter, D. Structure and dynamics of large ring polymers. *J. Rheol.* **2021**, *65*, 713−727.

(13) Halverson, J. D.; Kremer, K.; Grosberg, A. Y. Comparing the results of lattice and off-lattice simulations for the melt of nonconcatenated rings. *J. Phys. A: Math. Theor.* **2013**, *46*, No. 065002.

(14) Pasquino, R.; Vasilakopoulos, T. C.; Cheol Jeong, Y.; Lee, H.; Rogers, S.; Sakellariou, G.; Allgaier, J.; Takano, A.; Brás, A. R.; Chang, T.; Gooßen, S.; Pyckhout-Hintzen, W.; Wischnewski, A.; Hadjichristidis, N.; Richter, D.; Rubinstein, M.; Vlassopoulos, D. Viscosity of Ring Polymer Melts. *ACS Macro Lett.* **2013**, *2*, 874−878.

(15) Tu, M. Q.; Davydovich, O.; Mei, B.; Singh, P. K.; Grest, G. S.; Schweizer, K. S.; O'Connor, T. C.; Schroeder, C. M. Unexpected Slow Relaxation Dynamics in Pure Ring Polymers Arise from Intermolecular Interactions. *ACS Polym. Au* **2023**, *3*, 307−317.

(16) Doi, M.; Edwards, S. F. *The Theory of Polymer Dynamics*; Oxford Clarendon Press, 1989.
(17) Grosberg, A. Y.; Khokhlov, A. R. *Statistical Physics of Macromolecules*; AIP Press, 1994.
(18) Rubinstein, M.; Colby, R. H. *Polymer Physics*; Oxford University Press, 2003.
(19) de Gennes, P. G. *Scaling Concepts in Polymer Physics*; Cornell University Press: Ithaka, 1979.
(20) Strobl, G. R. *The Physics of Polymers*; Springer, 1997.
(21) Halverson, J. D.; Grest, G. S.; Grosberg, A. Y.; Kremer, K. Rheology of Ring Polymer Melts: From Linear Contaminants to Ring-Linear Blends. *Phys. Rev. Lett.* **2012**, *108*, No. 038301.
(22) Gooßen, S.; Brás, A. R.; Krutyeva, M.; Sharp, M.; Falus, P.; Feoktystov, A.; Gasser, U.; Pyckhout-Hintzen, W.; Wischnewski, A.; Richter, D. Molecular Scale Dynamics of Large Ring Polymers. *Phys. Rev. Lett.* **2014**, *113*, No. 168302.
(23) Richter, D.; Gooßen, S.; Wischnewski, A. Celebrating Soft Matter's 10th Anniversary: Topology matters: structure and dynamics of ring polymers. *Soft Matter* **2015**, *11*, 8535−8549.
(24) Kapnistos, M.; Lang, M.; Vlassopoulos, D.; Pyckhout-Hintzen, W.; Richter, D.; Cho, D.; Chang, T.; Rubinstein, M. Unexpected Power-Law Stress Relaxation of Entangled Ring Polymers. *Nat. Mater.* **2008**, *7*, 997−1002.
(25) Parisi, D.; Kaliva, M.; Costanzo, S.; Huang, Q.; Lutz, P. J.; Ahn, J.; Chang, T.; Rubinstein, M.; Vlassopoulos, D. Nonlinear Rheometry of Entangled Polymeric Rings and Ring-Linear Blends. *J. Rheol.* **2021**, *65*, 695−711.
(26) Farago, B.; Falus, P.; Hoffmann, I.; Gradzielski, M.; Thomas, F.; Gomez, C. The IN15 Upgrade. *Neutron News* **2015**, *26*, 15−17.
(27) Guenza, M. G. Localization of Chain Dynamics in Entangled Polymer Melts. *Phys. Rev. E* **2014**, *89*, No. 052603.
(28) Kimmich, R.; Fatkullin, N. Polymer Chain Dynamics and NMR. *Adv. Polym. Sci.* **2004**, *170*, 1−113.
(29) Kimmich, R.; Fatkullin, N. Self-diffusion studies by intra- and inter-molecular spin-lattice relaxometry using field-cycling: Liquids, plastic crystals, porous media, and polymer segments. *Prog. Nucl. Magn. Reson. Spectrosc.* **2017**, *101*, 18−50.
(30) Rössler, E.; Stapf, S.; Fatkullin, N. Recent NMR investigations on molecular dynamics of polymer melts in bulk and in confinement. *Curr. Opin. Colloid Interface Sci.* **2013**, *18*, 173−182.
(31) Gubaidullin, A.; Shakirov, T.; Fatkullin, N.; Kimmich, R. Spin-lattice relaxation dispersion in polymers: Dipolar-interaction components and short- and long-time limits. *Solid State Nucl. Magn. Reson.* **2009**, *35*, 147−151.
(32) Fatkullin, N. An Introduction to the Quantum Mechanics of Spin Systems. Detailed Presentation of the Most Fundamental Facts. (Elective Lecture Course for Advanced Students. Ilmenau, October-December 2023) *ResearchGate* DOI: 10.13140/RG.2.2.19292.56967.
(33) Fatkullin, N.; Gubaidullin, A.; Stapf, S. Features of polymer chain dynamics as revealed by intermolecular nuclear magnetic dipole-dipole interaction: Model calculations and field-cycling NMR relaxometry. *J. Chem. Phys.* **2010**, *132*, No. 094903.
(34) Kehr, M.; Fatkullin, N.; Kimmich, R. Deuteron and proton spin-lattice relaxation dispersion of polymer melts: Intrasegment, intrachain, and interchain contributions. *J. Chem. Phys.* **2007**, *127*, No. 084911.
(35) Ostrovskaya, I. K.; Fatkullin, N. F. The Effect of the End Segments on the Dynamics of a Polymer Melt: The Frequency Nature of the Effect and Possibility of Experimental Observation in the Free Induction Decay of Deuterons. *Polym. Sci., Ser. A* **2020**, *62*, 132−139.
(36) Ostrovskaya, I. K.; Fatkullin, N. F.; Körber, T.; Rössler, E. A.; Lozovoi, A.; Mattea, C.; Stapf, S. On the theory of deuteron NMR free induction decay of reptating polymer chains: Effect of end segment dynamics. *J. Chem. Phys.* **2020**, *152*, No. 184904.
(37) Lindt, K.; Mattea, C.; Stapf, S.; Ostrovskaya, I. K.; Fatkullin, N. F. The deuteron NMR Hahn echo decay in polyethylene oxide melts. *AIP Adv.* **2022**, *12*, No. 075219.
(38) Hövelmann, C. H.; Gooßen, S.; Allgaier, J. Scale-Up Procedure for the Efficient Synthesis of Highly Pure Cyclic Poly(ethylene glycol). *Macromolecules* **2017**, *50*, 4169−4179.
(39) Brás, A. R.; Goossen, S.; Krutyeva, M.; Radulescu, A.; Farago, B.; Allgaier, J.; Pyckhout-Hintzen, W.; Wischnewski, A.; Richter, D. Compact Structure and Non-Gaussian Dynamics of Ring Polymer Melts. *Soft Matter* **2014**, *10*, 3649−3655.
(40) Mittermaier, A.; Kay, L. E. New Tools Provide New Insights in NMR Studies of Protein Dynamics. *Science* **2006**, *312*, 224−228.
(41) Korzhnev, D. M.; Salvatella, X.; Vendruscolo, M.; Di Nardo, A. A.; Davidson, A. R.; Dobson, C. M.; Kay, L. E. Low-Populated Folding Intermediates of Fyn SH3 Characterized by Relaxation Dispersion NMR. *Nature* **2004**, *430*, 586−590.
(42) Camilles, M.; Link, S.; Balbach, J.; Saalwächter, K.; Krushelnitsky, A. Quantitative NMR study of heat-induced aggregation of eye-lens Crystallin proteins under crowding conditions. *Biochim. Biophys. Acta, Proteins Proteomics* **2018**, *1866*, 1055−1061.
(43) Lozovoi, A.; Mattea, C.; Fatkullin, N.; Stapf, S. Segmental Dynamics of Entangled Poly(ethylene oxide) Melts: Deviations from the Tube-Reptation Model. *Macromolecules* **2018**, *51*, 10055−10064.
(44) Fischer, E.; Kimmich, R.; Beginn, U.; Möller, M.; Fatkullin, N. Segment diffusion in polymers confined in nanopores: A fringe-field NMR diffusometry study. *Phys. Rev. E* **1999**, *59*, 4079−4084.
(45) Fetters, L. J.; Lohse, D. J.; Colby, R. H. Chain Dimensions and Entanglement Spacings. In *Physical Properties of Polymers Handbook*, 2nd ed.; Springer: New York, 2007, Chapter 25, pp 447−454.

https://doi.org/10.1021/acs.macromol.3c02360
Macromolecules 2024, 57, 3765−3775